Available online at www.sciencedirect.com
ScienceDirect
Physica B 403 (2008) 1848–1853
PHYSICA B
www.elsevier.com/locate/physb

Structure, optical and electrical properties of $Ge_{30}Sb_{10}Se_{60}$ thin films

K.A. Aly[a,*], A.M. Abousehly[a], M.A. Osman[b], A.A. Othman[b]

[a]Department of Physics, Faculty of Science, Al-Azhar University, Assiut, Egypt
[b]Department of Physics, Assiut University, Assiut, Egypt

Received 17 September 2007; received in revised form 16 October 2007; accepted 17 October 2007

Abstract

Amorphous $Ge_{30}Sb_{10}Se_{60}$ chalcogenide thin films were prepared onto cleaned glass substrates using thermal evaporation technique. The structure of the as-prepared films was confirmed to be amorphous using X-ray diffraction. The optical absorption coefficient (α) for the as-deposited films was calculated by using reflectance and transmittance measurements in the wavelength range 400–900 nm. The optical constants (refractive index (n) and the extinction coefficient (k)) were controlled by Murman's exact equations. The effects of annealing temperature in the temperature range 300–658 K on the optical and electrical properties of the as-prepared $Ge_{30}Sb_{10}Se_{60}$ thin films were discussed in details. It was found that both the optical band gap E_g^{opt} and the activation energy for electrical conduction ΔE_{dc} increase with increasing the annealing temperature up to the glass transition temperature (T_g), followed by a remarkable decrease with the increase of annealing temperature above T_g. The obtained results were interpreted on the basis of amorphous–crystalline transformations.

Keywords: Structure; Annealing; Evaporation; Optical properties; X-ray diffraction

1. Introduction

The amorphous chalcogenide thin films exhibit interesting optical properties such as the high refractive index n, good transmittance in the IR range [1]. Chalcogenide glasses are a recognized group of the inorganic glassy materials which always contain one or more of the chalcogen elements (S, Se or Te but not O) in conjunction with more electropositive elements (As, Sb and Bi) [2]. The knowledge of real and imaginary parts of complex refractive index, as a function of wavelength and thickness, is necessary to make effective use of these materials for optoelectronic devices [3,4], particularly as an antireflective coating [5]. The variation of refractive index with doping and growth parameters also provides the means to tailor the refractive index to any desired value required for use in filters [6].

The optical band gap E_g^{opt} is one of the most fundamental parameters of semiconductors, and its temperature dependence E_g^{opt} (T) is of considerable interest for both scientific and technological reasons. The values of E_g^{opt} were found to increase in chalcogenide films with increasing the annealing temperature up to the glass transition temperature T_g [7,8]. The value of the optical band gap E_g^{opt} of the as-prepared film was found to increase with increasing film thickness [9].

The electrical conduction in chalcogenide glasses have different conduction mechanisms that can be written as [10]

$$\sigma = \sigma_0 \exp\left(-\frac{\Delta E}{k_B T}\right) + \sigma_1 \exp\left(-\frac{E_1}{k_B T}\right) + \sigma_2 \exp\left(-\frac{E_2}{k_B T}\right). \quad (1)$$

The three terms arise from three different conduction mechanisms, in the first region ($\sigma_0 \exp(-\Delta E/k_B T)$) which is the high-temperature region the dominant mechanism is the band conduction through the extended states, where σ_0 is the pre-exponential factor, ΔE is the activation energy, K_B is the Boltzmann's constant and T is the absolute temperature. The second region ($\sigma_1 \exp(-E_1/k_B T)$) represents the hopping conduction via localized states. The third region ($\sigma_2 \exp(-E_2/k_B T)$) represents the hopping conduction near the Fermi level.

*Corresponding author. Fax: +00 20 88 325647.
E-mail address: kamalaly2001@yahoo.com (K.A. Aly).

0921-4526/$ - see front matter © 2007 Elsevier B.V. All rights reserved.
doi:10.1016/j.physb.2007.10.019

Street et al. [11] proposed that bulk glassy samples are chemically ordered and the evaporated films are partially chemically disordered and contain a fairly large fraction of homopolar bonds. When the evaporated films are annealed at the glass transition temperature T_g, the density of homopolar bonds decrease and the films approach the structure of the bulk glass.

The present study concerns with studying the effect of film thickness on the optical properties of $Ge_{30}Sb_{10}Se_{60}$ thin films and the annealing effects on both the optical and electrical properties of $Ge_{30}Sb_{10}Se_{60}$ thin films. X-ray diffraction was also carried out to determine the structural changes in these films.

2. Experimental details

$Ge_{30}Sb_{10}Se_{60}$ chalcogenide glass was prepared from Ge, Sb and Se elements with purity 99.999%. The proper amount for each material was then weighed and introduced into cleaned silica ampoule. To avoid the oxidation of the sample, the ampoule was evacuated to 10^{-6} Torr. The melting point of Ge is higher than the melting point of Sb or Se, therefore the ampoule was heated up to 1373 K with heating rate 5 K/min, then kept constant for 24 h and then quenched into ice-cold water to obtain homogeneous systems. Hand shaking of the constituent materials inside the ampoule was necessary for realizing the homogeneity of the composition. The amorphous structure of bulk ingots was confirmed using X-ray diffraction analysis (XRD). The glass transition temperature T_g was investigated using differential scanning calorimetry (DSC) Shimadzu TA-50 apparatus. $Ge_{30}Sb_{10}Se_{60}$ thin films were prepared by thermal evaporation of small ingot pieces onto cleaned glass substrates (microscope slides). The thermal evaporation process was performed by using a coating (Denton Vacuum 502 A) system, at a pressure of approximately 10^{-6} Torr. During the deposition process (at normal incidence), the substrates were suitably rotated in order to obtain films of uniform thickness. The film thickness as well as the evaporation rate was controlled using a quartz crystal monitor, Denton's model DTM-100. The film thickness is 90, 100, 150 and 300 nm, and the rate of the film deposition was 10 nm/s. The composition of the $Ge_{30}Sb_{10}Se_{60}$ thin films was determined using the energy dispersive spectroscopy analysis (Link Analytical EDS).

The transmittance (T) and reflection (R) at normal incidence for thermally evaporated $Ge_{30}Sb_{10}Se_{60}$ thin films onto non-absorbing substrate have been measured in the wavelength range (300–900 nm) using Shimadzu UV-2101PC double-beam spectrophotometer attached with PC data acquisition system. For studying the annealing effects, the films were put in a furnace (in vacuum 2×10^{-5} Torr) for 2 h in the temperature range 300–658 K.

The electrical conductivity measurements were carried out for films with evaporated gold planer electrodes (14×0.1 mm), using a conventional circuit involving a digital Keithley 617 C electrometer. The dc measurements were carried out in the temperature range 300–658 K.

3. Results

Fig. 1(a) shows DSC trace for the as-prepared $Ge_{30}Sb_{10}Se_{60}$ glasses recorded at heating rate ($\beta = 10$ K/min), the characteristic features of DSC curve indicate the

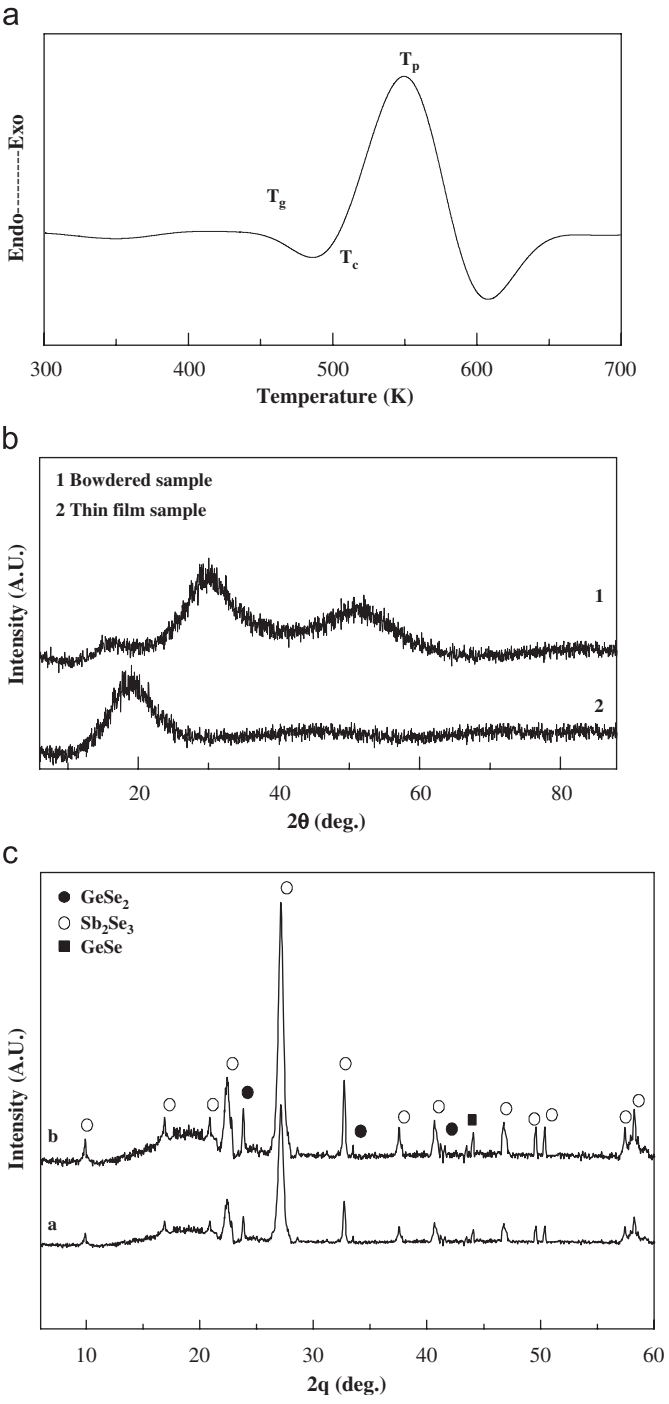

Fig. 1. (a) DSC trace for powdered $Ge_{30}Sb_{10}Se_{60}$ chalcogenide glass. (b) XRD of as-prepared $Ge_{30}Sb_{10}Se_{60}$ powdered glass (curve 1) and thin films (curve 2). (c) X-ray diffraction patterns for $Ge_{30}Sb_{10}Se_{60}$ thin films annealed at (a) 630 K and (b) 680 K.

homogeneity of the considered $Ge_{30}Sb_{10}Se_{60}$ glass. This may be confirmed by the appearance of one endothermic peak for $Ge_{30}Sb_{10}Se_{60}$ composition characterizing its glass transition temperature. Fig. 1(b) shows XRD of as-prepared $Ge_{30}Sb_{10}Se_{60}$ thin films and powdered glass. The general feature of these patterns confirms the amorphous nature of the bulk glass and the as-prepared films. In addition, $Ge_{30}Sb_{10}Se_{60}$ films are crystallized into different phases, Sb_2Se_3, $GeSe_2$ and GeSe, these phases have been identified using XRD patterns as shown in Fig. 1(c) for the annealed films at different annealing temperatures higher than the glass transition temperature.

Table 1 shows the spectral distribution of the constituent elements for the evaporated $Ge_{30}Sb_{10}Se_{60}$ thin films with film thickness 300 nm, it was found that the calculated compositions of the investigated films and those of the prepared compositions are very close to each other.

Fig. 2 shows the transmission spectra for as-prepared and annealed $Ge_{30}Sb_{10}Se_{60}$ thin films, respectively, at different annealing temperatures. It is observed that the optical transmission for $Ge_{30}Sb_{10}Se_{60}$ thin films increase (blue shift of the optical absorption edge) with increasing the annealing temperature up to the glass transition temperatures T_g and decrease (red shift of the optical absorption edge) with increasing the annealing temperature above this temperature.

Table 1
Spectral distribution of the constituent elements for $Ge_{30}Sb_{10}Se_{60}$ thin films with film thickness 300 nm

Element	Measured (at%)	Calculated (at%)	Difference
Ge	29.985	30	−0.015
Sb	10.016	10	0.016
Se	59.999	60	−0.001

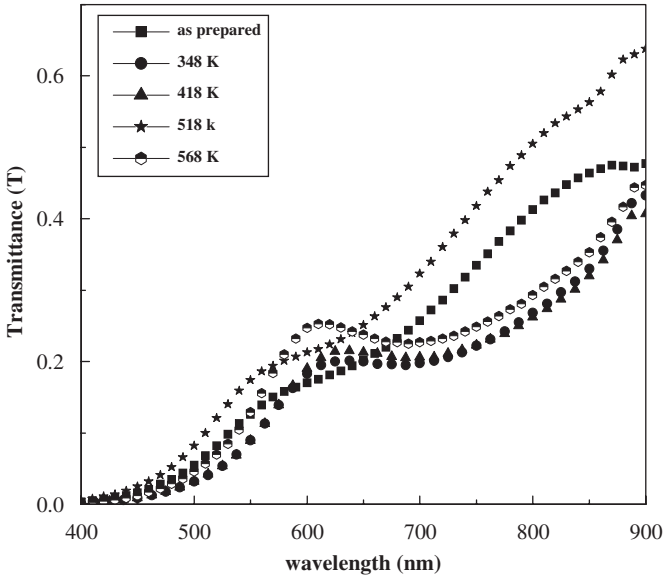

Fig. 2. Transmittance spectra for as-prepared and annealed $Ge_{30}Sb_{10}Se_{60}$ thin films.

For normal incidence measurements, the refractive index (n) and the extinction coefficient (k) were controlled by minimizing the errors ($\Delta R = R_{exp} - R_{cal}$, $\Delta T = T_{exp} - T_{cal}$) of the film using Murman's exact equations [12,13]. The analysis of the optical absorption data indicates that the optical band gap E_g^{opt} of these films obeys Tauc's [14] relation for the allowed non-direct transition:

$$\alpha(\lambda)h\nu = B(h\nu - E_g)^r, \tag{2}$$

where $h\nu$ is the photon energy, E_g is the optical band gap, B is an energy-independent constant (band-edge steepness parameter in Tauc's equation) and r is an integer or half-integer which determines the nature of optical transition ($r = 1/2$ for direct and $r = 2$ for non-direct transitions). Fig. 3(a) indicates that the plots of $(\alpha h\nu)^{1/2}$ vs. $h\nu$ for $Ge_{30}Sb_{10}Se_{60}$ thin films according to the power law [14] for non-direct allowed optical transition successfully describe the optical transitions in these films. Fig. 3(b) shows that the optical band gap E_g^{opt} for $Ge_{30}Sb_{10}Se_{60}$ thin films (300 nm) increase by increasing the annealing temperature up to the glass transition temperatures T_g followed by a remarkable decrease by increasing the annealing temperature above T_g. Fig. 4 represents the refractive index (n) as continuous function of wavelength (λ) for as-prepared and annealed $Ge_{30}Sb_{10}Se_{60}$ thin films. Fig. 5 represents the plots of $(\alpha h\nu)^{1/2}$ vs. $h\nu$ of $Ge_{30}Sb_{10}Se_{60}$ thin films with different film thicknesses. The real (ε_1) and imaginary (ε_2) parts of the complex dielectric constants can be written in the following forms [15,16]:

$$\varepsilon_1 = n^2 - K^2 = \varepsilon_\infty - \frac{e^2}{\pi c^2}\frac{N}{m^*}\lambda^2, \tag{3}$$

$$e^2 = 2nK, \tag{4}$$

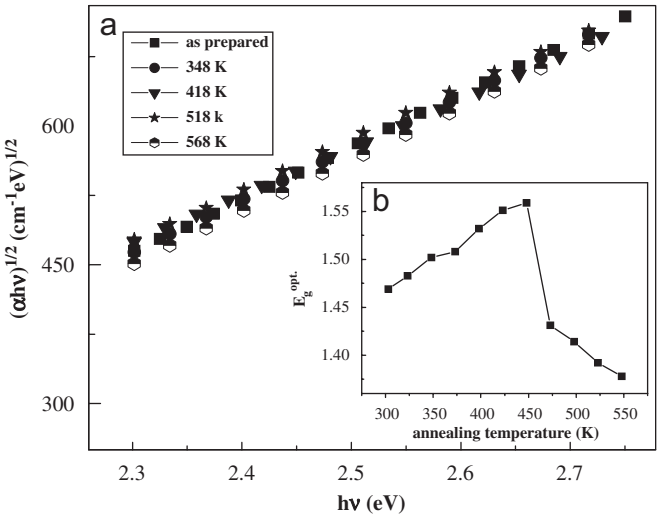

Fig. 3. (a) The plots of $(\alpha h\nu)^{1/2}$ vs. $h\nu$ for the as-prepared and annealed $Ge_{30}Sb_{10}Se_{60}$ thin films and (b) E_g^{opt} vs. annealing temperature for $Ge_{30}Sb_{10}Se_{60}$ thin films.

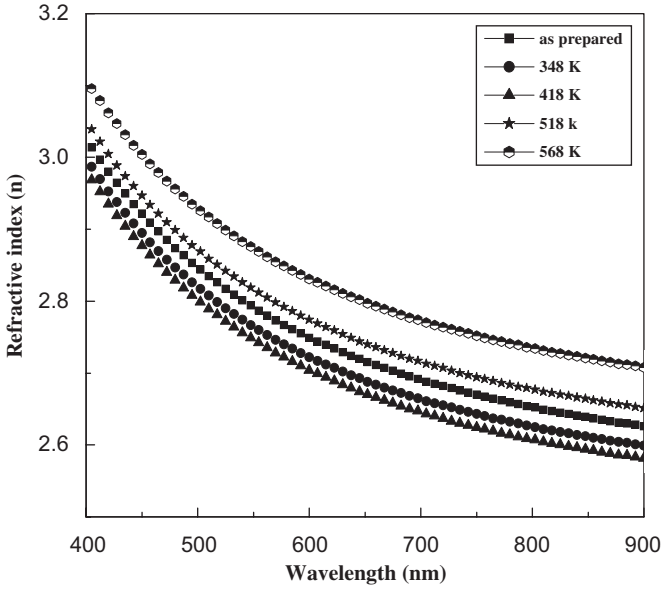

Fig. 4. The plots of refractive index (n) as a function of wavelength for as-prepared and annealed $Ge_{30}Sb_{10}Se_{60}$ thin films.

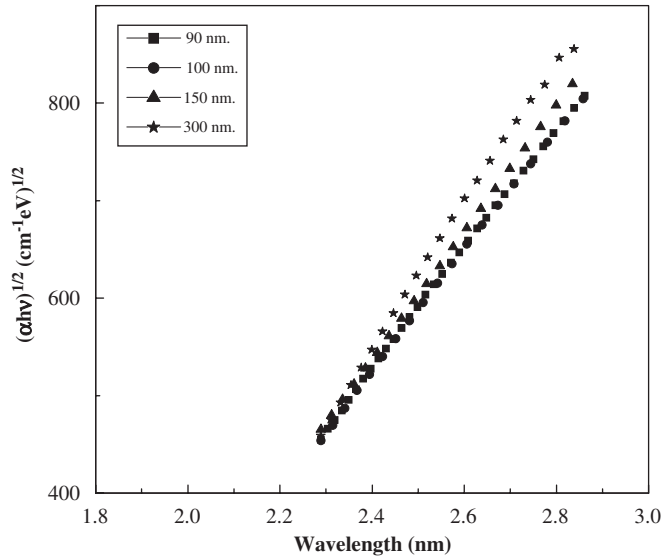

Fig. 5. The plots of $(\alpha h\nu)^{1/2}$ vs. $h\nu$ for $Ge_{30}Sb_{10}Se_{60}$ thin films with different thicknesses.

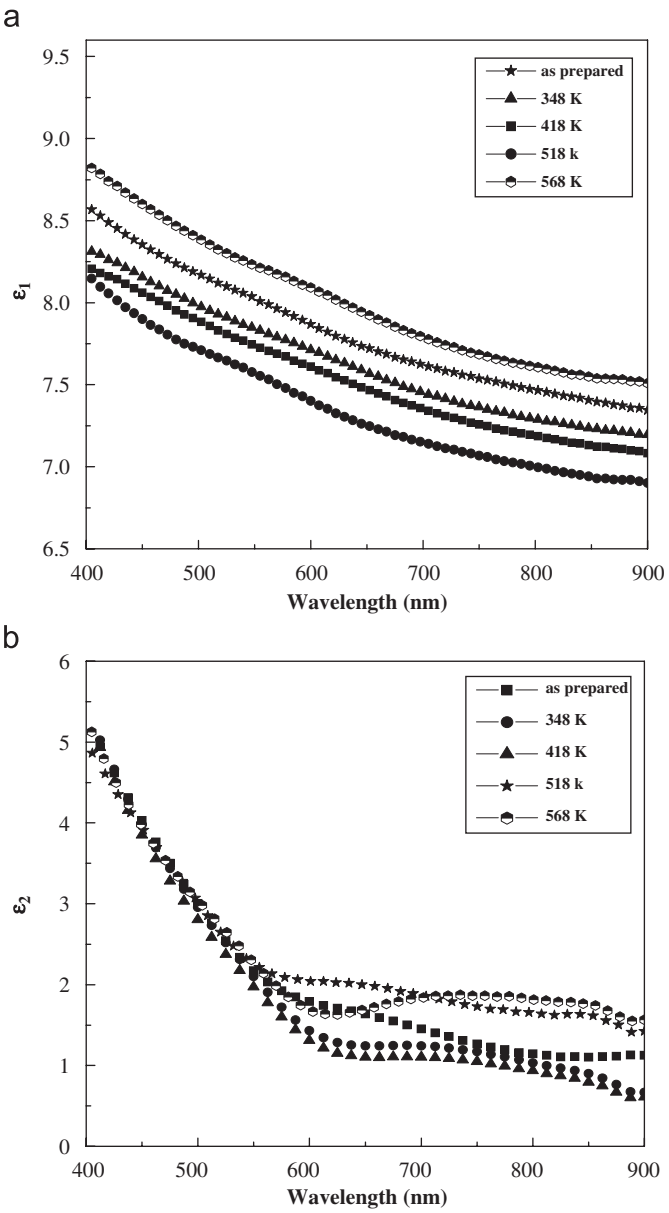

Fig. 6. The plots of (a) ε_1 vs. λ and (b) ε_2 vs. λ for as-prepared and annealed $Ge_{30}Sb_{10}Se_{60}$ thin films.

where ε_∞ is the high dielectric constant, e is the electronic charge, c is the velocity of light, (N/m^*) is the ratio of free carrier concentration (N) to the free carrier effective mass (m^*). This equation was employed to determine the parameters ε_∞ and (N/m^*) from the slope and intercept of the fitted straight lines of ε_1 vs. λ^2. Fig. 6(a) and (b) represents the variations of the real ε_1 and imaginary ε_2 parts of dielectric constants.

Among the most important parameters characterizing the optical materials as optical fibers can be determined from the energy dispersion of refractive index. Definitely, the n_0–photon energy relation has the following form [17,18]:

$$n_0^2(E) - 1 = \frac{E_d E_0}{E_0^2 - E^2}, \tag{5}$$

where $n_0(E)$ is the refractive index at photon energy $h\nu \to 0$, E_d is the electronic dispersion energy, E_0 is the single oscillator. From the slope and intercept of the fitted to straight lines of $[n_0^2(E) - 1]$ vs. E^2 dependence, one can determine the dispersion parameters $E_{d,}$ E_0 and n_0. Then, the variations of optical parameters (ε_∞, N/m^*, $E_{d,}$ E_0 and $n_{0)}$ were determined and tabulated in Table 2. The dependence of the dc conductivity on the annealing temperatures for $Ge_{30}Sb_{10}Se_{60}$ thin films is shown in Fig. 7(a) and the variations of the activation energy with annealing temperature for $Ge_{30}Sb_{10}Se_{60}$ thin films are

Table 2
The effect of annealing temperature T (K) on the optical parameters of $Ge_{30}Sb_{10}Se_{60}$ thin films with film thickness 300 nm

T (K)	ε_∞	N/m^* ($\times 10^{21}$ cm^{-3})	E_d (eV)	E_0 (eV)	n_0
323	8.750	1.5873	30.5195	5.34139	2.50986
343	8.539	1.5750	29.6953	5.36269	2.49992
368	8.312	1.5331	28.8301	5.37223	2.42984
393	8.307	1.5153	28.2425	5.38028	2.39331
418	8.448	1.5919	25.6053	5.35378	2.51402
443	8.512	1.6059	27.8053	5.3281	2.53199
468	8.694	1.6295	28.1239	5.30848	2.54324
493	8.746	1.6521	29.2070	5.30699	2.55864
518	8.833	1.6752	29.4946	5.29665	2.56195
543	9.027	1.7261	29.8358	5.22118	2.58311
568	9.123	1.7560	29.9013	5.18087	2.63963

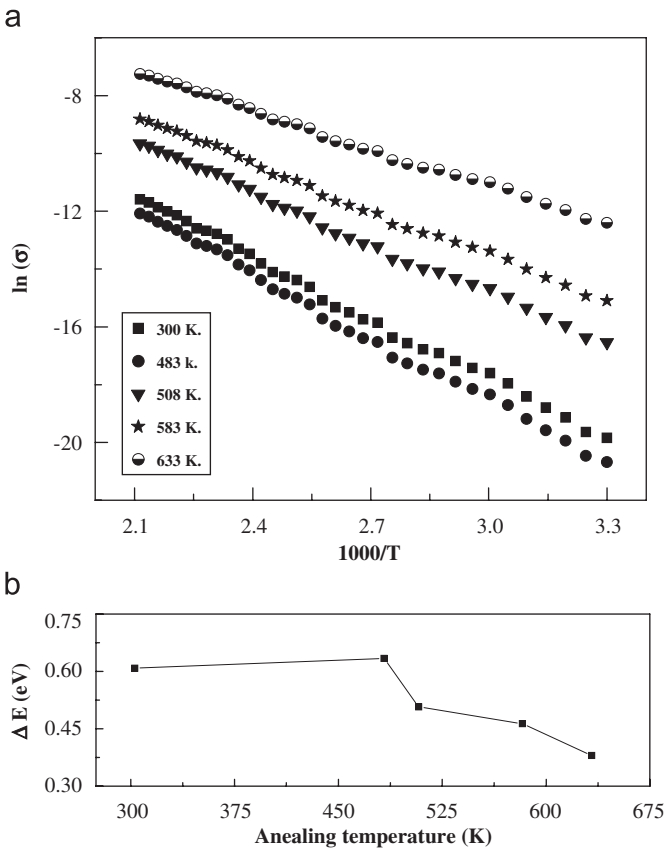

Fig. 7. (a) The plots of $\ln(\sigma)$ vs. $1000/T$. (b) The activation energy ΔE_{dc} vs. the annealing temperature for $Ge_{30}Sb_{10}Se_{60}$ thin films.

represented in Fig. 7(b). The behavior of ΔE_{dc} as that mentioned earlier for E_g^{opt} is the slight increase with increasing the annealing temperature up to T_g, then decrease with further increase of annealing temperature.

4. Discussion

Both the E_g^{opt} and ΔE_{dc} (see Figs. 3(b) and 7(b)) increase with increasing annealing temperature up to glass transition ($T_g = 478.76$ K), this behavior can be explained by the density of states model in amorphous solids proposed by Mott and Davis [19]. According to this model, the width of the localized states near the mobility edges depending on the degree of disorder and defects present in the amorphous matrix. The increase of annealing temperature up to T_g reduces the disorder and defects resulting in the reduction of the width of localized states in the band structure, consequently the optical band gap increase.

During annealing at temperatures higher than T_g the optical band gap decrease with increasing the annealing temperature. This behavior may be attributed to the producing of surface dangling bonds around the formed crystallites [20] during the process of crystallization. It has been suggested by many authors [20,21] that nearly ideal amorphous solids crystallize under heat treatment and that in the process of crystallization dangling bonds are produced around the surface of the crystallites. Further heat treatment causes the crystallites to break down [21] into smaller crystallites, thereby increasing the number of surface dangling bonds. These dangling bonds are responsible for the formation of some types of defects. These defects result in the decrease of the optical band gap E_g^{opt}. In the present work, the structure of as-prepared and annealed $Ge_{30}Sb_{10}Se_{60}$ thin films was examined using X-ray diffraction analysis (Fig. 1(b) and (c)). Continuous heat treatments at temperatures higher than T_g result in some crystalline phases defined by GeSe, $GeSe_2$ and Sb_2Se_3, which increase with increasing the annealing temperature. Thus, the major changes in the optical band gap could be ascribed to the thermally induced amorphous–crystalline transformations.

The high-frequency dielectric constant ε_∞ and the N/m^* ratio have the same manner which is opposite to that observed for E_g^{opt} (Table 2), also the refractive index (n_0) and dispersion energy (E_d) have the same manner which is opposite to that observed for E_0. These variations are strongly dependent on the internal microstructure change induced by heat treatment [22].

The film thickness approximately causes no changes (the changes within the experimental errors (see Fig. 5)) in the optical band gap in a-$Ge_{30}Sb_{10}Se_{60}$ thin films as well as those reported by Shaaban [23]. From Fig. 7(a), it can be observed that the dc conductivity (σ_{dc}) increase exponentially with the increase of temperature for $Ge_{30}Sb_{10}Se_{60}$ films. These results indicate that the conduction in these films is through an activated process having one conduction level and the dc conductivity (σ_{dc}) takes the formula $\sigma_{dc} = \sigma_0 \exp(\Delta E_{dc}/K_B T)$ (the first term of Eq. (1)), the calculated values of ΔE_{dc} for $Ge_{30}Sb_{10}Se_{60}$ films indicate that the conduction is due to thermally assisted tunneling of charge carriers in the localized states in the band tails [10]. It is observed that ΔE_{dc} values as well as E_g^{opt} values for $Ge_{30}Sb_{10}Se_{60}$ films "increase with the increase of annealing temperature up T_g followed by a monotonic decrease with further increase of annealing temperature above T_g". This behavior of ΔE_{dc} was previously discussed in details.

5. Conclusion

In the present study, the effect of annealing on the optical and electrical properties of $Ge_{30}Sb_{10}Se_{60}$ amorphous thin films has been investigated. We can concluded that annealing process at temperatures $T \leqslant T_g$ results in slightly increase in E_g^{opt} and ΔE_{dc}, whereas at $T > T_g$ the values of E_g^{opt} and ΔE_{dc} decrease with further increase of annealing temperature. The high-frequency dielectric constant ε_∞ and the N/m^* ratio have the same manner which is opposite to that observed toE_g^{opt}. Also, the refractive index (n_0) and dispersion energy (E_d) have the same manner which is opposite to that observed for E_0. The conduction in $Ge_{30}Sb_{10}Se_{60}$ thin films is ascribed to thermally activated conduction through the extended states that dominates in the temperature range 300–480 K. Finally, the film thickness approximately causes no changes in the optical properties of $Ge_{30}Sb_{10}Se_{60}$ thin films.

References

[1] L. Tichy, H. Ticha, P. Nagles, R. Callaerts, R. Mertens, M. Vlcek, Mater. Lett. 39 (1999) 122.
[2] A.H. Khafagy, M.S. Abo-Ghazala, M.M. El-Zaidia, A.A. El-Shourbagy, J. Non-Cryst. Solids 278 (2000) 119.
[3] Y. Tawada, K. Tsuge, M. Kondo, H. Okamoto, Y. Hamakawa, J. Appl. Phys. 53 (1982) 5273.
[4] H. Munckata, H. Kukimoto, Appl. Phys. Lett. 42 (1983) 432.
[5] J.C. Jans, J.W. Germmink, Appl. Opt. 32 (1993) 84.
[6] H.A. Maclcod, Thin Film Optical Filters, Adam Hilger/Macmillan, London, New York, 1987.
[7] J. Shirafuji, G.I. Kim, Y. Inuishi, J. Appl. Phys. 16 (1977) 67.
[8] M.A. Abdel-Rahim, A.H. Moharram, M. Dongel, M.M. Hafiz, J. Phys. Chem. Solids 51 (1990) 355.
[9] H.T. El-Shair, A.E. Bekheet, J. Phys. D 25 (1998) 1122.
[10] S.A. Fayek, M.H. El-Fouly, H.H. Amer, Solid State Commun. 93 (1995) 213.
[11] R.A. Street, R.J. Nemanich, G.A.N. Connell, Phys. Rev. B 18 (1978) 6915.
[12] O.S. Heavens, Optical Properties of Thin Solid Film, Butterworths, London, 1955.
[13] M.H. Liddell, Computer Aided Techniques for the Design of Multilayer Filters, Adam Hilger, Bristol, Boston, MA, 1981.
[14] J. Tauc, Amorphous and Liquid Semiconductors, Plenum, New York, 1974.
[15] S.A. Fayek, S.M. El-Sayed, NDT&E Int. 39 (2006) 39.
[16] R. Vahalova, L. Tichy, M. Vlcek, H. Ticha, Phys. Status Solidi A 181 (2000) 199.
[17] M. DiDomenijco, Appl. Opt. 11 (1972) 652.
[18] S.H. Wemple, M. DiDomenico, Phys. Rev. B 3 (1971) 1338.
[19] N.F. Mott, E.A. Davis, Electronic Process in Non-Crystalline Materials, Clarendon Press, Oxford, 1979.
[20] S. Chaudhuri, S.K. Biswas, J. Non-Cryst. Solids 54 (1983) 179.
[21] S. Hasegawa, M. Kitagawa, Solid State Commun. 27 (1978) 855.
[22] S.H. Wemple, Phys. Rev. B 7 (1973) 3767.
[23] E.R. Shaaban, Mater. Chem. Phys. 100 (2006) 411.